TARGET OF OPPORTUNITY MULTIPOINT IN SITU MEASUREMENTS WITH FALCONSAT-2

Dr. Linda Habash Krause
Assistant Research Professor, Department of Physics, U. S. Air Force Academy, CO

Dr. C. Lon Enloe
Professor, Department of Physics, U. S. Air Force Academy, CO

LtCol Ryan Haaland, Ph.D.
Assistant Professor, Department of Physics, U. S. Air Force Academy, CO

1.0 ABSTRACT

This paper describes the FalconSAT-2 mission objectives to take advantage of targets of opportunity to make multipoint *in situ* measurements of ionospheric plasma depletions simultaneously with other spacecraft. Because these plasma depletions are known to interfere with radio transmissions over a broad range of frequencies, including 100-1000 MHz, the international space weather community is investigating the instigation, temporal evolution, and spatial propagation of these structures in the hopes that a prediction tool may be developed to warn operators of outages in communications or navigation. FalconSAT-2 will be launched into a low altitude (360 km), medium inclination (52 degrees) orbit with sensors designed to measure *in situ* suprathermal plasma spectra at a rate of 10 samples per second. The primary mission objectives are to 1) investigate F region ionospheric plasma depletion morphology relative to geomagnetic activity, and 2) demonstrate the utility of the Miniature Electrostatic Analyzer (MESA) in measuring energy-resolved spectra of ionospheric electrons over a dynamic range such that plasma density depletions down to 0.1% of the background may be resolved at a rate of 10 Hz. Simultaneous *in situ* multipoint observations of ionospheric plasma depletions are designated as a secondary objective since FalconSAT-2 consists of a single spacecraft, and opportunities to make these simultaneous measurements with other spacecraft in compatible orbits are not in our control. Both deep and shallow bubbles, frequently observed in the pre- and post-midnight sectors, respectively [*Singh at al., 1997*], are known to exhibit magnetic field-aligned behavior [Fagundes et al., 1997]; thus, there is the expectation (to first order) that multiple spacecraft entering a magnetic flux tube simultaneously have the opportunity to observe a depletion structure at different points within the structure. This observation would provide insight into the plasma depletion extent along the field line. Other conjunction types, such as non-simultaneous intersection of a flux tube or crossing of orbital paths simultaneously in different magnetic flux tubes, provide insight into other aspects of depletion structure, such as constraining the plasma depletion extent and propagation speed along the magnetic field line, or plasma depletion vertical extent. With this paper, a statistical analysis of the probability that FalconSAT-2 will intersect a magnetic flux tube during eclipse simultaneously with other spacecraft capable of measuring thermal electrons is presented.

2.0 INTRODUCTION

Observations of physical properties of the space environment often rely on systems fixed in space to investigate temporal evolution of various processes (*e.g.*, ground based imaging) or systems that move through space to investigate slowly-varying spatial structures (*e.g.*, satellites or rockets.) Furthermore, certain properties of the space environment are more readily accessible through *in situ* measurements (*e.g.*, the variability of particle energy distributions in small scale structures, three-dimensional imaging of neutral wind divergence) than remote sensing. Time series data analysis assists in separating temporal from spatial effects [*Song and Russell, 1999*.] However, for synoptic scale phenomena that span very large areas, such as coupling effects between the high latitude and low latitude ionospheres, simultaneous multipoint measure-ments offer insight into processes that connect the two regions. For example, *Šafránková et al.* [1998]

used multipoint measurements of solar wind and magnetopause properties (*e.g.*, dynamic pressure, ion density, magnetic field) to assess the impact of abrupt changes in solar wind dynamic pressure on magnetopause motion and to determine the speed of the interplanetary shock as it passed through the magnetopause. More specific to the topic of interest in our present study, *Indiresan* et al. [1998] used dual-point measurements of plasma density and drift taken from the Tethered Satellite System (TSS-1R) to demonstrate that vertically coherent structured plasma depletions can exist within independent magnetic flux tubes.

Options for providing space vehicles to conduct such multipoint measurements include satellite constellations, formation flying, and tethered satellites, but these methods often require large expenditures on multiple spacecraft, sophisticated design processes, or advanced technologies (*e.g.*, Microelectromechnical Systems (MEMS) for a CubeSAT-like formation.) The U. S. Air Force Academy's FalconSAT-2 mission relies on a less complicated, less expensive solution by launching a single satellite with the expectation that there will be multipoint opportunities with other satellites at certain times. However, this requires the ability to determine when those opportunities will arise, requiring detailed knowledge of both the orbital states of the satellites and a rough understanding of the target phenomenon to be studied. Presently, we are particularly interested in making simultaneous multipoint measurements of ionospheric equatorial plasma depletions. These structures tend to originate near the equator at night and often upwell to higher altitudes and propagate along magnetic field lines [*Fagundes et al., 1997*.] So, to first order, they reside within magnetic flux tubes. With this approximation, we have developed a model combining orbital mechanics and magnetic field specification to determine the times at which multiple-satellite conjunctions of a single flux tube occur. A list of potential targets of investigation using these measurements appears in Table 1.

The paper is organized as follows: Section 3 provides the background on the effects of equatorial plasma depletions, the FalconSAT-2 mission, and other missions developed to investigate equatorial plasma depletions. Model development theory and procedures are presented in Section 4, with results and validation appearing in Section 5. Section 6 provides an analysis of opportunities for multipoint measurements with FalconSAT-2 and other spacecraft, with a recommendation for specifying orbital parameters to maximize these opportunities. Concluding remarks and recommendations for future work appear in Section 7.

Table 1. Opportunities for investigation based upon type of conjunction.

Conjunction	Target of Investigation
FSII and C/NOFS simultaneously intersect a magnetic flux tube at different latitudes	Plasma bubble extent along the field line
FSII and C/NOFS non-simultaneously intersect a magnetic flux tube at different latitudes	Constraint on plasma bubble extent and propagation speed along the field line
Orbital paths cross simultaneously in different magnetic flux tubes	Plasma bubble vertical extent
Orbital paths cross in the same magnetic flux tube and the satellites arrive non-simultaneously	Local plasma bubble temporal evolution
Orbital paths cross in the different magnetic flux tubes and the satellites arrive non-simultaneously	Constraint on plasma bubble vertical extent and propagation speeds

3. IONOSPHERIC PLASMA DEPLETIONS

Plasma is a dispersive medium with a unique relationship between the charged particle density and the index of refraction. Communication systems that require propagation through the ionosphere rely on signals with frequencies either high enough to avoid reflection and absorption, such as those required for earth-space links, or low enough to take advantage of reflections off of specific layers in the ionosphere, such as those used in long range ground communication or ionospheric sounding. However, when there are severe spatial anisotropies in the plasma density, especially on the scale of the first Fresnel zone unique to signal frequency and range, then the signal may experience differential refraction that could lead to phase or amplitude scintillation of the signal. Since plasma bubbles affect signals of frequencies from HF to K-band and everything in between, this is of obvious concern to organizations that increasingly rely on space systems as an integral component of their infrastructure. As a result, a good deal of research is being conducted to understand the nature of plasma depletions, leading to a prediction capability that would assist in the development of system failure mitigation techniques.

Signal fluctuations due to a disturbed medium can result in either phase or amplitude scintillation. The severity of amplitude scintillation is often characterized by the S_4 parameter:

$$S_4^2 = \frac{\langle I^2 \rangle - \langle I \rangle^2}{\langle I \rangle^2}$$

where I is the signal intensity. As an example, a value of $S_4 = 0.45$ corresponds to a signal fade of 10 dB. Climatological models have been developed to provide average behavior of plasma depletions and the associated scintillation activity. In particular, Wideband Model (WBMOD) can be used to specify signal fading of a user-specified signal frequency, location of origination, and range to receiving station (*e.g.*, altitude of satellite.) In addition, the user may specify various levels of solar and geomagnetic activity. An example of WBMOD computations for VHF scintillation experienced during times of high solar activity appears in Figure 1. For this run, the frequency is 250 MHz, the signal is transmitted from a ground station at 0° latitude and 0° longitude, and the receiving satellite is at geosynchronous altitudes. The color bar denotes the S_4 parameter, and the purple line represents the day/night terminator, with the dark shading representing night. Note that the bulk of the scintillation occurs near the equator shortly after sunset. Areas with no data indicate areas in which there was no line of sight between the ground station and the satellite.

The Air Force Research Laboratory and the Department of Defense's Space Test Program are presently developing a mission called the Communications/Navigation Outage Forecasting System (C/NOFS), a satellite with a sophisticated set of plasma and neutral environment sensors to provide data used in the development of an operational warning and mitigation system. The idea is to use ground based and satellite observations in conjunction with empirical and physics-based models to provide a scintillation nowcasting and forecasting system. Data from other satellites are useful in developing physics based models, especially if they can be related in time or space.

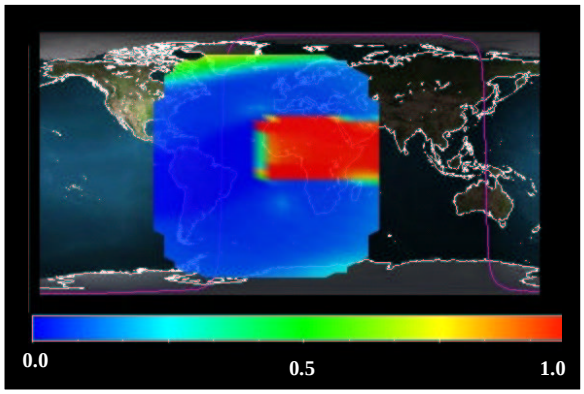

Figure 1. S_4 is computed for VHF signals during high solar activity. See text for details.

FalconSAT-2 is a student-built microsatellite designed for launch from the Space Shuttle Get-Away Special (GAS) canister [*Habash Krause et al., 2001*]. The satellite will be launched into a 360 km circular orbit at an inclination of 52° and has a payload of plasma sensors sensitive enough to detect plasma depletions of severity up to 1000 times below ambient density. In particular, the Miniature Electrostatic Analyzer (MESA) is a patch sensor configured to measure electron spectra differential in energy from cold (with pre-acceleration) up to 10 eV. An image of MESA appears in Figure 2, and details of the instrument design and performance are found in [*Enloe et al., 2002.*]

Other missions that have contributed to our understanding of plasma depletions include the Defense Meteorological Satellite Program (DMSP) constellation, Atmospheric Explorer, and Taiwan's ROCSAT-1. All of these, with the

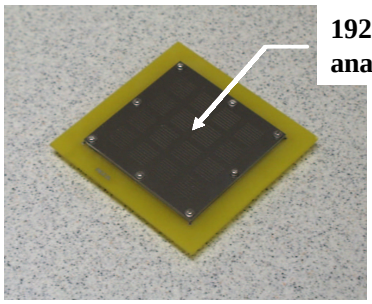

Figure 2. The Miniature Electrostatic Analyzer (MESA) is the primary instrument to measure electron spectra with FalconSAT-2.

exception of Atmospheric Explorer, are still in operation as of the time of writing this paper. With the launch of FalconSAT-2 potentially in January 2003 and that of C/NOFS the following November, there is a possibility of having up to seven or eight satellites in orbits that may experience one or more of the various types of conjunctions outlined in Table 1. Specific satellite parameters are presented in Section 6, which covers the analysis of opportunities to make multipoint measurements of various types.

4. MODEL DEVELOPMENT

Our model to predict the conjunctions of spacecraft with magnetic flux tubes consists of two primary components: an orbital mechanics model and magnetic field model.

4.1 Modeling Orbital Mechanics

A flowchart of Orbital Mechanics model appears in Figure 3. Keplerian elements are initialized at the simulation start time t_{START}, and initial state vectors $\vec{r}$ and $\vec{v}$ are computed. Certain Keplerian elements are allowed to vary, such as the true anomaly ν, the argument of perigee ω, and the longitude of the ascending node Ω. The magnitude of the eccentricity vector $\vec{e}$ is constant, though its direction is variable. The mean and eccentric anomalies (*M* and *E*, respectively) are computed as a function of time, and state vectors are computed using updated values of ω and Ω. Latitude and longitude values are then computed, and the simulation is repeated until the end time t_{END} is reached. Governing equations are provided below.

The theoretical treatment of orbital mechanics is presented in several well-written texts [*e.g.*, Bate *et al.*, 1971, Vallado, 1997] and a review of the fundamental equations that were used in development of the model are presented here.

Given radii of apogee r_a and perigee r_p, the semi-major axis *a* and the scalar eccentricity *e* are given by:

$$a = \frac{r_a + r_p}{2} \qquad e = \frac{r_a - r_p}{r_a + r_p} \tag{1}$$

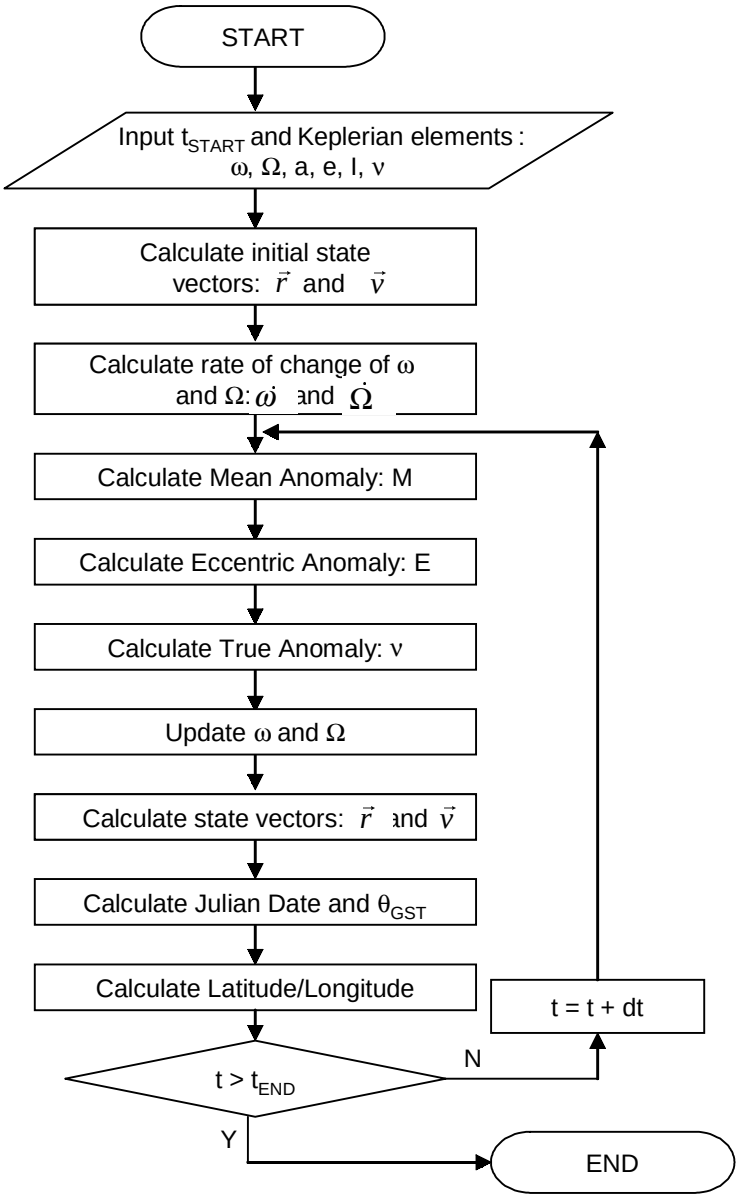

Figure 3. Flowchart for the astrodynamics model algorithm. See text for a detailed description.

Then the semi-parameter *p* and the gravitational parameter μ are given by:

$$p = a\left(1 - e^2\right) \tag{2}$$

$$\mu = 3.986 \times 10^5 \text{ km}^3/(\text{solar sec})^2$$

For inclination *i* defined as the angle between the orbit and equatorial planes, we can compute the constant rate of change of ω and Ω. These represent the rotation of the line of apsides and nodal regression due to the Earth's equatorial

bulge, respectively, and may be computed from the following:

$$\dot{\omega} = \frac{3}{2}\frac{J_2 R_0 \mu}{a^{3/2}\left(1-e^2\right)^2}\left(2-\frac{5}{2}\sin^2 i\right)$$

$$\dot{\Omega} = \frac{-2.38247\times10^{13}}{a^{7/2}}\cos(i) \qquad (3)$$

where J_2 = 0.0010826269 and R_0 is the Earth's mean radius = 6378.1316 km.

Then, the mean, eccentric, and true anomalies are computed as a function of time:

$$M = t\sqrt{\frac{\mu}{a^3}}$$

$$E \cong M + \frac{e\sin M}{1-e\cos M} - \frac{1}{2}\left(\frac{e\sin M}{1-e\cos M}\right)^3$$

$$\tan\frac{\nu}{2} = \left(\frac{1+e}{1-e}\right)^{1/2}\left(E - e\sin E\right) \qquad (4)$$

The state vectors are then computed in the perifocal coordinate system:

$$\vec{r}_{PER} = \begin{bmatrix} \frac{p\cos(\nu)}{1+e\cos(\nu)} \\ \frac{p\sin(\nu)}{1+e\cos(\nu)} \\ 0 \end{bmatrix}$$

$$\vec{v}_{PER} = \begin{bmatrix} -\sqrt{\frac{\mu}{p}}\sin(\nu) \\ -\sqrt{\frac{\mu}{p}}\left(e+\cos(\nu)\right) \\ 0 \end{bmatrix} \qquad (5)$$

The state vectors are then transformed into the geocentric coordinate system using the relation $\vec{r}_{GEO} = [\mathrm{T}]\vec{r}_{PER}$, where [T] is a transformation matrix given by:

$$[\mathrm{T}] = \begin{bmatrix} \cos\Omega\cos\omega - \sin\Omega\sin\omega\cos i & -\cos\Omega\sin\omega - \sin\Omega\cos\omega\cos i & \sin\Omega\sin i \\ \sin\Omega\cos\omega + \cos\Omega\sin\omega\cos i & -\sin\Omega\sin\omega - \cos\Omega\cos\omega\cos i & \cos\Omega\sin i \\ \sin\omega\sin i & \cos\omega\sin i & \cos i \end{bmatrix}$$

Once these were found, it was a straightforward process to compute the latitude and longitude of the spacecraft. Note that all references to time are in solar units. First, one must compute the Julian Date JD_0, defined as the number of days since 12:00 1 January 4713 B.C.:

$$JD_0 = 367y - \mathrm{int}\left\{\frac{7}{4}\left[y + \mathrm{int}\left(\frac{m+9}{12}\right)\right]\right\} + \mathrm{int}\left(\frac{275m}{9}\right) + d + \ldots$$

$$+\frac{h}{24} + 1{,}721{,}013.5$$

where y is the year, m is the month, d is the day, and h is the fractional hour. Then, we find T_{UT1}, the number of centuries since 1 Jan 2000:

$$T_{UT1} = \frac{JD_0 - 2{,}451{,}545}{36{,}525} \qquad (8)$$

Then the Greenwich sidereal time since 1 Jan 00:00 of the year θ_{GST0} is given by:

$$\theta_{GST0} = 1.753368560 + 628.3319706889T_{UT1} + \ldots$$
$$+ 6.7707\times10^{-6}T_{UT1}^2 - 4.5\times10^{-10}T_{UT1}^3 \qquad (9)$$

Greenwich sidereal time is then given by:

$$\theta_{GST} = \theta_{GST0} + \omega_{\oplus}UT1 \qquad (10)$$

where $\omega_{\oplus}$ is the Earth's angular rotation rate (in rad/s), and UT1 is the universal time in solar seconds.

Then, with the help of the right ascension α, given by $\cos(\alpha) = x/\sqrt{(x^2+y^2)}$, we can find the longitude λ and (geocentric) latitude ϕ as:

$$\lambda = \alpha - GST$$

$$\phi = \tan^{-1}\left(\frac{z}{\sqrt{x^2+y^2}}\right) \qquad (11)$$

The above set of equations provides enough information to compute the latitude and longitude of a spacecraft given its initial Keplerian elements. Other parameters, such as the eccentricity vector or line of nodes, may be easily derived with identity formulas provided in fundamental texts [*e.g.*, Vallado, 1997.]

4.2 Modeling Magnetic Flux Tubes

A magnetic flux tube is an abstract, somewhat subjective concept often used to characterize space environment phenomena that happen to be field aligned. Here, we apply the term to specify tubes containing field-aligned plasma depletions. As the plasma depletions upwell, they grow in spatial extent. This, coupled with a magnetic field that weakens with increasing altitude, provides the impetus to designate flux tubes that increase in altitude thickness with increasing altitude. Conversely, we expect the flux tube thickness to decrease with increasing latitude due to magnetic field convergence toward the poles. Using a non-tilted dipole, we computed flux tubes for the altitude range from 390 km to 1480 km at the equator. The equation of magnetic field lines for a non-tilted dipole is given by:

$$r(r_{eq},\theta) = r_{eq}\sin^2\theta \qquad (12)$$

where θ is the colatitude (π/2-latitude). The flux tubes were constructed such that their inner and outer radii followed dipole magnetic field lines, and the outer shell of one flux tube is collocated with the inner shell of the next highest flux tube. Latitude ranged from 0° to 30° in 2° increments. A plot of the flux tubes used in this study appears in Figure 4.

Plasma depletions are known to be 10s of km wide in longitude, so the 360° longitude range was divided into 50 km segments. Thus, a typical flux tube at an equatorial altitude of 500 km may be 150 km by 50 km (altitude and longitude, respectively) and extend along the entire magnetic field line. (In reality, the plasma depletions tend to decay such that we may consider the base of the F region – around 150-200 km in altitude – as the "endpoints" of the plasma depletion. Since none of the satellites considered here will reach that low in altitude, we do not explicitly truncate the flux tube at the base of the F region.)

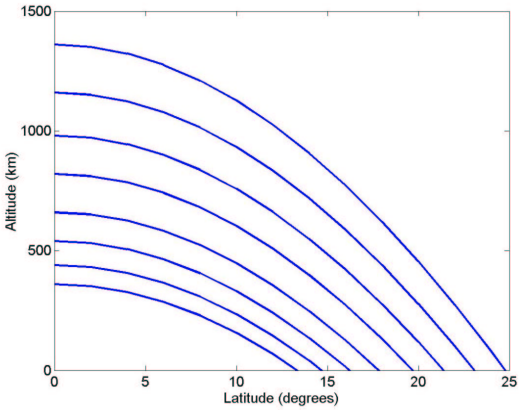

Figure 4. Magnetic Flux Tubes are computed for the altitude range of interest in this study.

Two criteria are necessary to specify a conjunction:

1. the satellites are within 50 km of each other in longitude
2. the satellites are within a maximum altitude separation relative to a flux tube defined for that altitude.

Criterion number 1 is necessary for longitude conjunctions, whereas both criteria 1 and 2 are necessary for flux tube conjunctions.

For example, let's say that FS2 and C/NOFS are within 50 km of each other in longitude. We would then map their positions down the magnetic field lines to the equator and compute the equatorial radii for both spacecraft. If the difference between the equatorial radii is less than the thickness of the equatorial flux tube assigned to that altitude, then criterion number 2 is satisfied and there is a flux tube conjunction. Results are presented in the following section.

5. MODEL RESULTS AND VALIDATION

First, we present orbital simulation results using a set of spacecraft Keplerian elements appropriate for FalconSAT-2. The orbit is circular of altitude 360 km, the inclination is 52°, and the longitude of the ascending node is 120°. The individual components of the position and velocity vectors are plotted as a function of time in Figures 5 and 6. Next, we repeat the process for C/NOFS and

DMSP, with DMSP results appearing in Figure 7. Finally, as an example of the validation process, we compare the results for FalconSAT-2 latitude from our model and AF-GEOSpace (see Figures 8 and 9.)

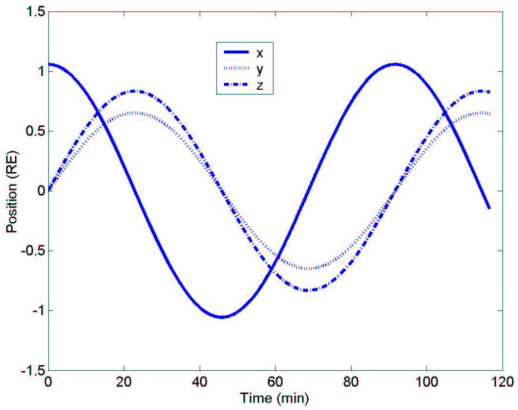

Figure 5. FalconSAT-2 Position components.

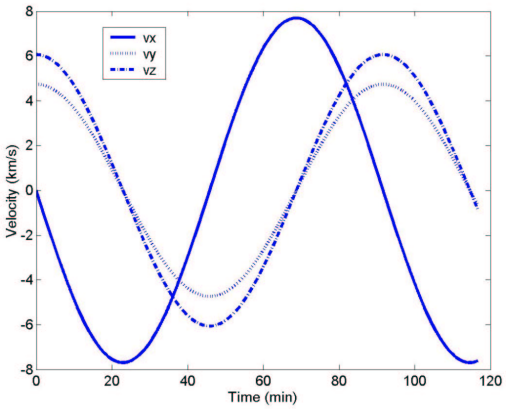

Figure 6. FalconSAT-2 Velocity Components.

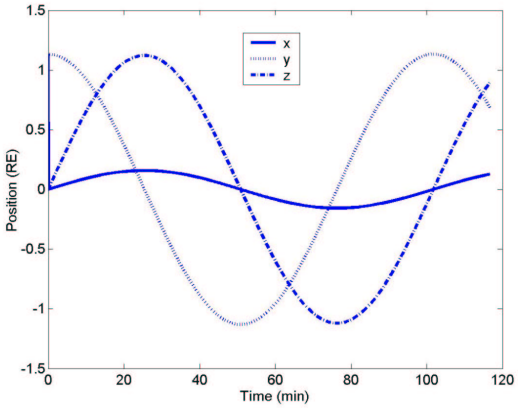

Figure 7. DMSP Position Components.

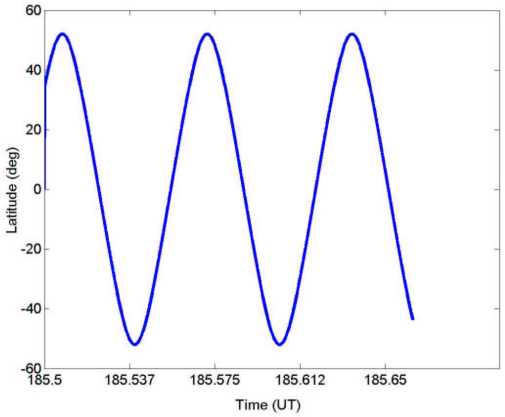

Figure 8. FS2 Latitude from USAFA model.

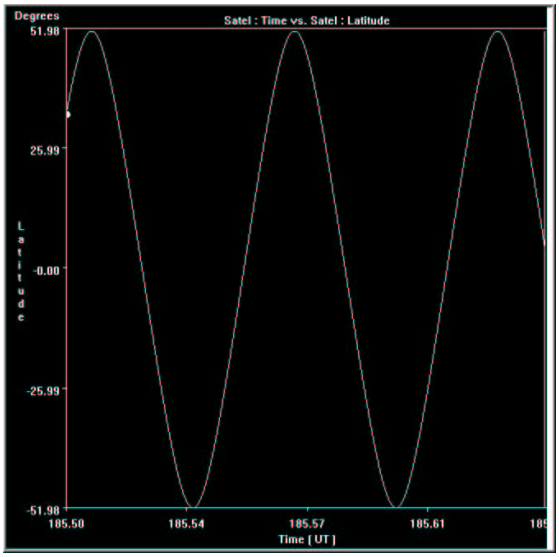

Figure 9. FS2 latitude from AF-GEOSpace.

From our validation efforts, we have determined complete consistency of our calculations of state vectors with those produced by AF-GEOSpace for both prograde and retrograde orbits. However, it turns out that while the GEOSpace longitude plots are identical in shape to those produced by the USAFA model, there is an offset in time. Nonetheless, since this offset is uniform for all cases, we are confident that our model can be used to determine flux tube conjunctions, though more work needs to be accomplished to determine the geographic longitude of the conjunctions.

6. COMPUTING CONJUNCTIONS

In modeling the FalconSAT-2 conjunction opportunities, we use the Keplerian elements specified in the previous section and compare conjunction opportunities with C/NOFS and DMSP. Not all Keplerian elements were available, so we took liberty in varying some of the unknown parameters to investigate the effects on the opportunities.

First, we begin with an analysis of opportunities for conjunctions with C/NOFS. This is a 400 km by 700 km orbit of 13° inclination. We assume the following: $\Omega = 105°$ and $\omega = 45°$. With these parameters, our model found 268 seconds of longitude conjunction time within a 28 hour time, with 69 of those resulting in magnetic flux tube conjunctions. A plot showing two pairs of coordinates appears in Figure 10. The red markers denote a flux tube conjunction, whereas the green markers denote a longitude conjunction.

Then, we examined the possibility of conjunctions between FS2 and DMSP. Though we found several longitude conjunctions (311 seconds in 28 hours,) not one flux tube conjunction was detected. In fact, the equatorial separation radius was virtually uniform, around 480 km, corresponding to the difference in orbital radii. This confirms that circular orbits are perhaps not best suited for maximizing the probability of flux tube conjunctions. Although C/NOFS is

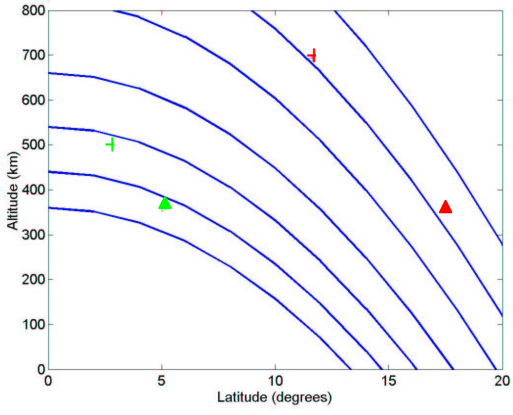

Figure 10. C/NOFS (+) and FS-2 (triangle) for two longitude conjunctions, with one of these (red) resulting in a magnetic flux tube conjunction.

eccentric, similar results were found for C/NOFS and DMSP conjunction opportunities – only longitude conjunctions were found.

7. CONCLUDING REMARKS

From our computations of longitude and flux tube conjunction times for FalconSAT-2, C/NOFS, and DMSP, we have demonstrated that the FalconSAT-2 and C/NOFS orbits are most likely to experience flux tube conjunctions than other combinations of spacecraft considered here. The DMSP sun-synchronous circular orbit and the FalconSAT-2 circular orbit of 52° inclination provide opportunities for longitude conjunctions, but the only opportunities for flux tube conjunctions would take place when DMSP is near the equator and FalconSAT-2 is at a higher latitude. This requires precise specification of the FalconSAT-2 spacecraft Keplerian elements – an option unavailable to us as a secondary payload. Though the computations for DMSP and C/NOFS did not reveal flux tube conjunctions, a long-term analysis needs to be completed to determine opportunities throughout their multi-year mission durations.

In addition to the need for multipoint measurements to investigate ionospheric plasma depletion structure and evolution, there have been other investigators that have stated a need for such measurements to answer questions on the validity of competing space physics theories [e.g., *Lockwood, 1997.*] With tools such as these, scientists are able to more effectively use resources that are already in place.

REFERENCES

Bate, R. D., D. D. Mueller, and J. E. White, *Fundamentals of Astrodyamics*, Dover, New York, 1971.

Enloe, C. L., L. Habash Krause, R. K. Haaland, T. Patterson, C. Richardson, C. Lazidis, Miniaturized electrostatic analyzer manufactured using photolithographic etching, *Rev. Sci. Instrum.*, submitted, 2002

Fagundes, P.R., Y. Sahai, Y., I. S. Batista, J. A. Bittencourt, M. A. Abdu, and H. Takashi, Vertical and zonal equatorial F-region plasma bubble

velocities determined from OI 630 nm nightglow imaging, *Adv. Space Res., v20*, n6, p 1297-1300, 1997

Habash Krause, L., C. L. Enloe, R. K. Haaland, A Nanosatellite Mission to Investigate Equatorial Ionospheric Plasma Depletions: The U. S. Air Force Academy's FalconSat-2, *SSC01-VIIIa-7, Proc. 15th Annual Small Satellite Conference*, Logan, Utah, 2001.

Indiresan, R. S., B. E. Gilchrist, S. Basu, J. -P. Lebreton, and E. P. Szuszczewicz, Simultaneous, dual-point, in situ measurements of ionospheric structures using space tethers: TSS-1R observations, *Geophys. Res. Lett., v. 25*, n. 19, 3725-3728, 1998.

Lockwood, M., Testing Substorm Theories: The Need for Multipoint Observations, *Adv. Space Res., v. 20*, n. 4-5, 883-894, 1997.

Safrankova, J., Z. Nemecek, L. Prech, G. Zastenker, K. I. Paularena, N. Nikolaeva, M. Nozdrachev, A. Skalsky, and T. Mukai, January 10-11, 1997 Magnetic Cloud: Multipoint Measurements, *Geophys. Res. Lett., v. 25*, n. 14, 2549-2552, 1998.

Singh, S., D. K. Bamgboye, J. P. McClure, and F. S. Johnson, Morphology of equatorial plasma bubbles, *J. Geophys. Res., v. 102*, n. A9, 20,019-20,030, 1997

Song, P. and C. T. Russell, Time Series Data Analyses in Space Physics, *Space Sci. Rev., v. 87*, pp. 387-463, 1999.

Vallado, D. A., *Fundamentals of Astrodynamics* and Applications, Space Technology Series, McGraw-Hill, New York, 1997.